ACS Macro Letters

Letter

pubs.acs.org/macroletters

Controlling the Location of Nanoparticles in Polymer Blends by Tuning the Length and End Group of Polymer Brushes

Hyun-Joong Chung,[†,§] Jinyong Kim,[†,∥] Kohji Ohno,[‡] and Russell J. Composto*[,†]

[†]Department of Materials Science and Engineering and Laboratory for Research on the Structure of Matter, University of Pennsylvania, Philadelphia, Pennsylvania 19104-6272, United States

[‡]Institute for Chemical Research, Kyoto University, Uji, Kyoto 611-0011, Japan

Supporting Information

ABSTRACT: This paper investigates controlling the location of nanoparticles (NPs) in a phase-separated polymer blend of deuterated poly(methyl methyl methacrylate) (dPMMA) and poly(styrene-*ran*-acrylonitrile) (SAN). Silica NPs are grafted with PMMA brushes having molecular weights of 1800, 21000, and 160000 at fixed grafting density. Using ion beam milling combined with SEM imaging, NP location and morphology are investigated for blends containing 10 wt % NP. With increasing brush length, the NPs are found to segregate to the dPMMA/SAN interface, partition between the interface and dPMMA phase, or locate in the dPMMA phase, respectively.

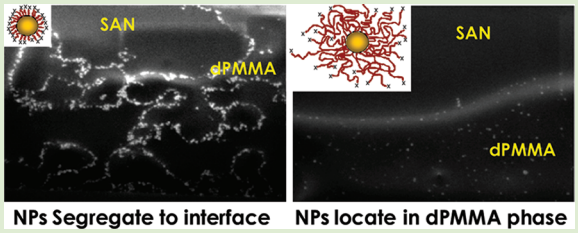

Adding nanoparticles (NPs) to a polymer matrix is a promising way to create novel nanocomposites with enhanced strength, conductivity, permeability, catalytic activity, optical, and magnetic properties.[1] If the matrix contains multiple components, such as in a polymer blend, these properties will depend on the precise location of NPs within or between phases. For about a hundred years, particles have been used to stabilize emulsions by a mechanism call Pickering stabilization.[2−11] Here, oil-and-water emulsions are stabilized by colloidal particles that segregate to the interface between two immiscible liquids. More recently, the self-assembly of NPs in block copolymers[1,12−23] and polymer blends[24−39] has attracted much attention because they can direct structure formation from the nanoscale to mesoscale. A comprehensive review article by Balazs et al. summarizes this field of research.[40] Understanding how NP type, shape, size and surface functionalization controls their location in multiphase polymers will greatly improve our ability to manipulate and direct the structure of both block copolymers and blends. For example, NPs that selectively locate in one phase can slow down structural evolution in polymer blends by increasing the viscosity,[28] whereas NPs that jam at the interface between immiscible phases can stabilize a bicontinuous structure.[24−41] Recently, a jamming morphology map was constructed to show how polymer blend film thickness and NP concentration determined whether the morphology was discrete or bicontinuous.[42] In the present study, we aim to control nanoparticle location in a phase separated polymer blend by varying the length and end-group of polymer brushes grafted to silica NPs.

The interfacial energy that controls the location of NPs in polymer blends (α/β) differs in magnitude from oil-and-water emulsions. If particle flocculation and entropic terms are neglected, the criterion for locating NPs at the α/β interface is

$$|\sigma_{\alpha/NP} - \sigma_{\beta/NP}| < \sigma_{\alpha/\beta} \quad (1)$$

where σ is the interfacial energy.[43] On the contrary, NPs locate in the α (β) phase if $\sigma_{\alpha/NP} < \sigma_{\beta/NP}$ ($\sigma_{\alpha/NP} > \sigma_{\beta/NP}$). In typical oil−water emulsions, $\sigma_{\alpha/\beta}$ values range from 10 to 50 mJ/m^2. Thus, particle location can be readily controlled by varying the hydroxyl (hydrophilic) and methyl (hydrophobic) groups on the particle surface.[2,3] However, because most polymer blends consist of hydrophobic components, $\sigma_{\alpha/\beta}$ is typically very small, about 1 mJ/m^2. Therefore, subtle changes in the NP surface functionality can be used to guide NPs to either the interface between immiscible polymers or into one of the phases. Such control is difficult to achieve with oil−water emulsions because the interfacial energy between phases dominates.

Recent studies have investigated how brush type and surface attachment chemistry controls the interfacial activity and location of NPs in block copolymers. For example, Kim et al.[21] showed that small changes in thiol end group chemistry can drive polystyrene (PS) coated Au NPs from the PS domains to the interface when dispersed in a symmetric poly(S-*b*-2-vinylpyridene), P(S-*b*-2VP), diblock copolymer. These results were attributed to a high areal chain density, 2.4 chains/nm^2, for brushes grafted by a primary thiol end group versus a low areal density, 1.3 chains/nm^2, when attachment is via a sterically hindered, secondary thiol. These researchers were also able to control the location of AuNPs by varying the brush composition using a random copolymer of PS and P2VP, and areal density. Costanzo and Beyer[22] were able to

Received: September 13, 2011
Accepted: December 27, 2011
Published: December 30, 2011

   dx.doi.org/10.1021/mz200068p | *ACS Macro Lett.* 2012, 1, 252−256

manipulate the location of AuNPs after their incorporation into a symmetric P(S-*b*-methyl methacrylate), P(S-*b*-MMA), copolymer. Here, the NPs were decorated with a diblock copolymer brush containing a polyethylene glycol outer block joined to a PS inner block via a Diels–Alder linkage that cleaves above 90 °C. Initially, upon solvent annealing the NPs located in the PMMA domains of the lamella in P(S-*b*-MMA) and then, after thermal treatment, the linkage cleaved and the PS grafted NPs migrated toward the interface to reduce the unfavorable enthalpic interactions with the PMMA domain. Huang et al.[23] also used thermal degradation of ligands attached to Au NPs to control their location in a spherical PS-*b*-P4VP copolymer.

For block copolymers containing NPs, the guideline posed by eq 1, solely based on interfacial energies, is insufficient because the conformational entropy of the block can play a dominant role in determining NP location.[1] In polymer blends containing NPs, however, this entropic penalty does not play a significant role because the size scale of the phase separated domains (>hundreds of nanometers) is much greater than the radii of gyration of the polymers. Therefore, eq 1 provides a useful guiding principle.

In this paper, we demonstrate that the location of NPs dispersed in a phase-separated polymer blend can be tuned by varying the brush length and end group. The polymer matrix is a 50:50 mixture of deuterated poly(methylmethacrylate) (dPMMA) and poly(styrene-*ran*-acrylonitrile) (SAN). Using atom transfer radical polymerization (ATRP), silica nanoparticles are modified with Cl terminated PMMA brushes having molecular weights (M_n) of 1800, 21000, and 160000. We have previously investigated the morphological evolution of polymer blend films containing nanoparticles.[24,42,44] In this paper, these PMMA-grafted NPs are denoted as P2K, P21K, and P160K, respectively. Using focused ion beam milling and SEM imaging, the NP location and morphology are investigated. The NPs are homogeneously distributed in the as-cast films. Upon annealing at 195 °C, the polymer blends undergo phase separation to dPMMA-rich and SAN-rich phases (denoted as dPMMA and SAN). As brush length increases, the NPs are observed to segregate to the dPMMA/SAN interface, partition between the interface and dPMMA phase, or locate in the dPMMA phase, respectively. Correspondingly, the morphology evolves from a bicontinuous structure to macroseparated domains. Replacing hydrogen with deuterium in the PMMA matrix does not influence the location of the NPs in the phase separated structure. Upon replacing the Cl terminal group of the brush with H (i.e., dehalogenation), NPs with the shortest brush partition between the interface and dPMMA phase. The effect of brush length and end group termination on NP location is consistent with the entropic and enthalpic contributions originating from the conformation of grafted brushes and the density of chain-end groups on the brush, respectively.

Effect of Grafted Chain Length. The location of NPs in a phase-separated blend will depend on the interactions between the NP and each phase relative to a NP segregated to the interface (i.e., adsorption energy). After FIB milling to form a trench, SEM was used to determine the blend morphology and the location of NPs at the wall of the trench. In order to apply thermodynamic models to explain the multiphase system, the particles must be shown to be predominantly isolated and uniformly dispersed in as-cast samples (i.e., well-defined starting state). At a NP concentration of 10 wt %, Figure 1

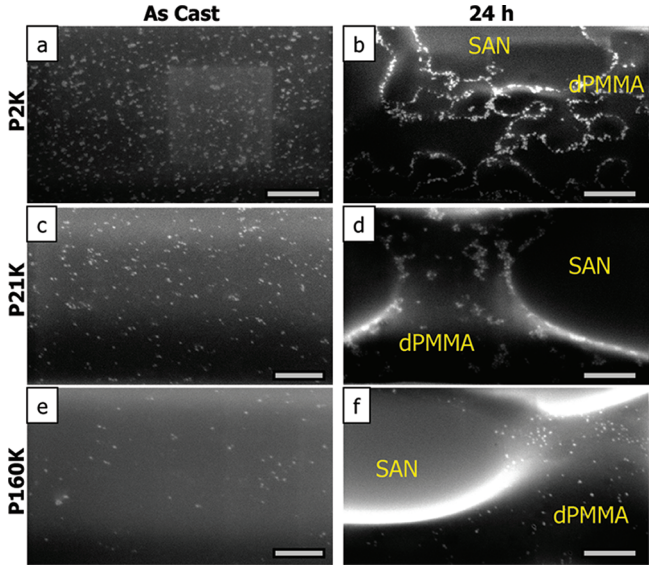

Figure 1. Cross-sectional SEM images of dPMMA:SAN films containing 10 wt % of P2K (a, b), P21K (c, d), and P160K (e, f). Initially, NPs are homogeneously dispersed in one-phase mixtures (a,c,e). Upon annealing for 24 h at 195 °C, dPMMA and SAN phase-separate and, consequently, P2K segregates to the interface between dPMMA and SAN phases (b), P21K partitions between the interface and dPMMA phase and (d), P160K locates in the dPMMA phase (f). Scale bars are 500 nm.

shows that (a) P2K, (c) P21K, and (e) P160K are homogeneously distributed in the as-cast films. Note that only the silica particles, and not the brush, appear in the SEM images. Using the grafting density and M_n's of the brushes, the volume fractions occupied by the silica core decreases strongly with brush length, namely 57.9%, 10.3%, and 1.6% for P2K (P2K–H), P21K, and P160K, respectively.

The brush length of the PMMA-grafted NPs controls the location of the NPs in the phase-separated dPMMA:SAN blends. In Figure 1b, the P2K NPs are observed to segregate to the interface between the dPMMA and SAN domains. This result is consistent with our prior studies that show P2K NPs jam at the interface between domains, resulting in a frozen bicontinuous or discrete morphology.[24,42] Block copolymer micelles have also been observed to locate at an interface[45,46] suggesting that "hard" NPs and "soft" micelles can act as surfactants under the proper conditions. To test the effect of deuteration, a PMMA:SAN film was prepared having 10 wt % of P2K. After 24 h at 195 °C, the P2K segregated to the interface (not shown), indicating that the deuterium of PMMA does not affect the interfacial activity of the P2K NPs. Upon increasing the brush length from 2K to 21K, the NPs are found to partition between the interface (~33%) and dPMMA phase as shown in Figure 1d. For dPMMA:SAN containing 20 wt % P21K, the same partitioning of NPs was observed at 4 h and 24 h. (See Supporting Information). As the brush length increases to 160k, the NPs locate mainly within the dPMMA domain as shown in Figure 1f. In summary, PMMA grafted NPs tend to segregate to the interface between the dPMMA and SAN phases when the PMMA brush is short, whereas longer brushes result in NPs that locate in the dPMMA phase.

Contact Angles of NP Films. Because the interfacial energies between the NP and PMMA (SAN) are unknown, we have indirectly determined the surface energy of the NPs as a function of brush length in order to qualitatively predict their

dx.doi.org/10.1021/mz200068p | *ACS Macro Lett.* 2012, 1, 252–256

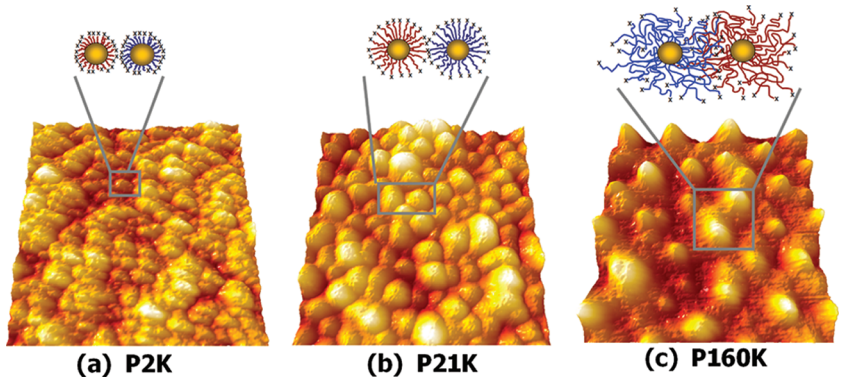

Figure 2. AFM surface topography images (1 μm × 1 μm) of NP films containing P2K (a), P21K (b), and P160K (c). Schematic cartoons above each image represent the chain conformations for each particle and end group X (X = Cl or H). The nearest-neighbor, center-to-center distance between NPs are 22 ± 9, 52 ± 15, and 101 ± 28 nm for parts a–c, respectively.

location in a phase separated blend. The surface energies were estimated by measuring the water contact angle on films containing only NPs (i.e., no matrix polymer) deposited on silicon. For a water (W) drop forming a contact angle (θ) on a NP film, the Young equation is

$$\cos\theta = \frac{\sigma_{NP/A} - \sigma_{NP/W}}{\sigma_{A/W}} \quad (2)$$

where A represents air and $\sigma_{A/W}$ is 71.9 mJ/m^2.[3] For NP films consisting of P2K, P21K, and P160K (cf. Figure 2), θ decreases from 84.0 ± 0.7°, to 72.0 ± 1.2° to 69.2 ± 0.7°, respectively. These results indicate that the films become more hydrophilic as the PMMA brush length increases. For comparison, the water contact angle on a PMMA film is 69.8 ± 0.3°, which is the same as the P160K film. This result suggests that the long brush of PMMA on the P160K NPs have a similar surface energy as pure PMMA (i.e., no chain end effects). In contrast, P2K films, which consist of NPs with a short PMMA brush, exhibit a larger contact angle relative to PMMA (i.e., chain end effect increases hydrophobicity). Thus, the contact angle results support the experimental findings that show that P160K NPs locate in the PMMA phase whereas the P2K NPs segregate to the interface. These results suggest that the enthalpic penalty for P160K to disperse in PMMA is less than that of P2K. Namely, the interfacial tension between the longer brush in P160K and PMMA is much smaller than that between the shorter brush in P2K and PMMA. Not surprisingly, films of P21K exhibit a contact angle of 72.0°, which lies between the P160K and P2K values. Consistent with the surface energy of these intermediate length brushes, the P21K NPs are found at both the interface and within the PMMA phase in phase separated blends.

Entropic and Enthalpic Considerations. The surface properties of P2K and P21K films (i.e., covered with PMMA brush) differ from pure PMMA. For example, when added to dPMMA/SAN, P2K, and P21K segregate entirely or partially to the interface, as shown in Figure 1, indicating that the PMMA brush interacts somewhat unfavorably with the dPMMA phase. Furthermore, the water contact angles on P2K and P21K films are greater than the PMMA film suggesting that the surface energies of the NPs are greater than PMMA. This increase in surface energy can be attributed to (i) an extended brush conformation (entropic) and/or (ii) a high density of "unfavorable" end groups (enthalpic).

To investigate the role of brush conformation, AFM was used to characterize the NP films . As shown in Figure 2, the boundaries surrounding the P2K (Figure 2a) and P21K (Figure 2b) NPs are relatively sharp with each NP retaining a nearly spherical shape. This hard sphere-like appearance is consistent with a dry brush where interpenetration is limited and the brushes are stretched as noted in the cartoons above Figure 2, parts a and b. These images suggest that the high surface energy of the shorter brushes, P2K and P21K NPs, results from conformational restrictions at high grafting density. However, for the P160K film shown in Figure 2c, the PMMA brush regions between silica cores (yellow) are flat and smooth, indicating that the brushes can interpenetrate. To quantify this observation, the stretching of the bush was calculated from the nearest neighbor distances, 22 ± 9, 52 ± 15, and 101 ± 28 nm, respectively. From small-angle X-ray scattering, the number average silica diameter is 12.8 nm.[47] Using these values, the brush thicknesses, h, are 4.6, 19.6, and 44.1 nm, respectively. The degree of stretching relative to the unperturbed radius of gyration, h/R_g, can be calculated for the longer brushes where Gaussian statistics apply for the homopolymer. For the P21K NPs, h/R_g is 3.8, which is greater than the value of 3.1 determined for P160K NPs. This smaller value for the P160K NPs is consistent with interpenetration of neighboring brushes and/or less stretching for the longer brush. With increasing brush length, the transition from an extended, short brush to a collapsed, longer brush with more conformational freedom suggests a weakening of 'wetting autophobicity',[48,49] an observation that is consistent with the contact angle values, θ(PMMA) ≅ θ(P160K) and θ(PMMA) < θ(P2K).

The chain end density can be estimated from the center-to-center distance between neighboring NPs. Using the silica diameter of 12.8 nm and a brush grafting density of 0.7 chains/nm^2, the number of chain ends per volume is calculated and decreases rapidly from 6.4 × 10^{-2} to 4.9 × 10^{-3} to 6.7 × 10^{-4} /nm^3 as brush length increases. The cartoon in Figure 2 is meant to capture this reduction in chain end density, denoted as X. These calculations do not account for the effect of matrix interpenetration on brush height.[49] Nevertheless, the significantly greater chain end density for short brushes may account for the higher surface energies of P2K and P21K. Moreover, because the chain end density for P160K is low, chain ends will have a much smaller effect on the surface energy (relative to P2K and P21K), consistent with the similar contact angles for the P160K film and PMMA .

dx.doi.org/10.1021/mz200068p | ACS Macro Lett. 2012, 1, 252–256

Effect of Chain End Groups. Chain end groups may contribute to an enthalpic interaction between NPs and the surrounding matrix. For P2K, P21K, and P160K, the PMMA brushs are terminated with Cl. To understand whether chain ends provide a discernible enthalpic contribution, P2K NPs were dehalogenated to produce a H terminated analog denoted as P2K−H. For P2K−H films, the water contact angle was only 72.0 ± 1.2° compared with the P2K value of 84.0 ± 0.7°, indicating that P2K−H NPs are more wettable than P2K. To test this observation, P2K−H at 10 wt % were added to dPMMA:SAN films and annealed for 24 h at 195 °C. In contrast to the P2K case, the P2K−H partition between the interface and dPMMA phase as shown in Figure 3. Although this partitioning is similar to the behavior of P21K, the P2K−H NPs tend to form larger aggregates in the dPMMA phase suggesting that they are less miscible than P21K.

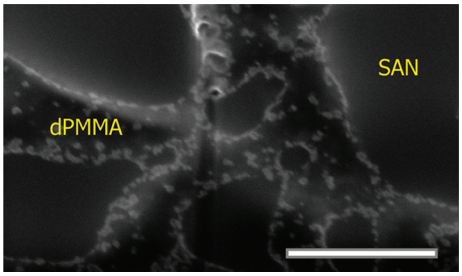

Figure 3. Cross-sectional SEM images of dPMMA:SAN films containing 10 wt % P2K−H after annealing at 195 °C for 24 h. The P2K−H NPs partition between the interface and the dPMMA phase, suggesting that the hydrogen-terminated NPs are more miscible with PMMA than the chlorine-terminated P2K.

NPs grafted with identical brushes of the same chain length but differing in termination group can exhibit different surface properties. For P2K and P2K−H, contact angle and morphology (Figure 3) studies suggest that NPs terminated with H are more hydrophilic and more miscible with PMMA than Cl terminated brushes. The effect of chain ends on the matrix-brush interaction is likely related to their different atomic parameters. For example, the van der Waals radii, atomic polarizability, and electronegativity values of Cl and H are 1.75 vs 1.2 Å, 2.18 vs 0.667 $Å^3$, and 3.16 vs 2.20, respectively.[50] We hope that these insights, along with surface segregation studies of end terminated polymers[51] spark the development of theories that can accurately determine the surface energy of polymer-grafted NPs. Once the surface energy of polymer-grafted NPs can be precisely determined by theory and/or experiment, eq 1 can be used to accurately predict where the NPs will locate in polymer blends . This insight can also be used to design polymer brushes to control NP location. In addition, this advance would allow technologists to direct the location of NPs in other heterogeneous polymer systems such as block copolymers.

In this paper, we demonstrate that the location of polymer-grafted NPs in polymer blends depends on both the chain length and end group of the brush. For short (P2K), intermediate (P21K), and long (P160K) brushes, silica NPs segregate to the interface, partition between the interface and dPMMA phase, and locate in the dPMMA phase, respectively. The P2K, P21K, and P160K NPs are all terminated with Cl. To understand the role of chain ends, a hydrogen-terminated analog of P2K (P2K−H) is prepared and found to partition between the interface and dPMMA phase. Water contact angle values confirm that the surface energy of NPs depend on brush chain length and end group. The NP location can now be predicted by knowing the interfacial energies between NP and matrix polymers. Surface and interfacial energy of polymer grafted NPs are determined by chain conformation (entropic) and the density and the species of end groups (enthalpic). We hope that these results motivate future theoretical studies aimed at controlling the location of NPs in polymer blends and block copolymers.

■ ASSOCIATED CONTENT

Supporting Information

Additional FIB pictures and detailed experimental methods. This material is available free of charge via the Internet at http://pubs.acs.org.

■ AUTHOR INFORMATION

Corresponding Author

*E-mail: composto@seas.upenn.edu.

Present Addresses

[§]University of Illinois at Urbana−Champaign

[∥]KCC Corporation, Korea

Author Contributions

H.-J.C and R.J.C. designed experiments and wrote the manuscript. H.-J.C., J.K, and O.K. performed the experiments. All authors have given approval to the final version of the manuscript.

Notes

The authors declare no competing financial interest.

■ ACKNOWLEDGMENTS

This work was supported by the National Science Foundation with primary support from the Polymer (DMR09-07493), MRSEC(DMR05-20020), and MWN (DMR0908449) programs. We acknowledge facility support for AFM and FIB/SEM from the NSF/NBIC program (08-32802) and PENN Regional Nanotechnology Facility, respectively.

■ REFERENCES

(1) Bockstaller, M. R.; et al. *Adv. Mater.* **2005**, *17*, 1331.
(2) Aveyard, R.; Binks, B. P.; Clint, J. H. *Adv Colliod Interf Sci* **2003**, *100−102*, 503.
(3) Binks, B. P.; Clint, J. H. *Langmuir* **2002**, *18*, 1270.
(4) Subramaniam, A. B.; et al. *Nat. Mater.* **2005**, *4*, 553.
(5) Velev, O. D.; et al. *Langmuir* **1996**, *12*, 2374.
(6) Stancik, E. J.; et al. *Langmuir* **2004**, *20*, 90.
(7) Dinsmore, A. D.; et al. *Science* **2002**, *298*, 1006.
(8) Wang, H.; Hobbie, E. K. *Langmuir* **2003**, *19*, 3091.
(9) Vignati, E.; et al. *Langmuir* **2003**, *19*, 6650.
(10) Simovic, S.; Prestidge, C. A. *Langmuir* **2004**, *20*, 8357.
(11) Saleh, N.; et al. *Langmuir* **2005**, *21*, 9873.
(12) Huh, J.; et al. *Macromolecules* **2000**, *33*, 8085.
(13) Lee, J. Y.; et al. *Macromolecules* **2002**, *35*, 4855.
(14) Thompson, R. B.; et al. *Science* **2001**, *292*, 2469.
(15) Tsutsumi, K.; et al. *Langmuir* **1999**, *15*, 5200.
(16) Lopes, W. A.; Jaeger, H. M. *Nature* **2001**, *414*, 735.
(17) Lin, Y.; et al. *Nature* **2005**, *434*, 55.
(18) Yeh, S. W.; Chang, Y. T.; Chou, C. H.; Wei, K. H. *Macromol. Rapid Commun.* **2004**, *25*, 1679.
(19) Chiu, J. J.; et al. *J. Am. Chem. Soc.* **2005**, *127*, 5036.
(20) Reister, E.; et al. *Macromolecules* **2004**, *37*, 4718.
(21) Kim, B. J.; et al. *Macromolecules* **2007**, *40*, 1796.
(22) Constanzo, P. J.; et al. *Macromolecules* **2007**, *40*, 3996.

(23) Huang, C.-M.; et al. *Macromolecules* **2007**, *40*, 5067.
(24) Chung, H. J.; et al. *Nano Lett* **2005**, *5*, 1878.
(25) Ginzburg, V. V.; et al. *Phys. Rev. Lett.* **1999**, *82*, 4026.
(26) Tang, Y. L.; Ma, Y. Q. *J. Chem. Phys.* **2002**, *116*, 7719.
(27) Laradji, M.; MacNevin, G. *J. Chem. Phys.* **2003**, *119*, 2275.
(28) Chung, H. J.; et al. *Europhys. Lett.* **2004**, *68*, 219.
(29) Vermant, J.; et al. *Rheol. Acta* **2004**, *43*, 529.
(30) Minelli, C; et al. *Colloid Polym. Sci.* **2004**, *282*, 1274.
(31) Tanaka, H.; et al. *Phys. Rev. Lett.* **1994**, *72*, 2581.
(32) Steinmann, S.; et al. *Polymer* **2002**, *43*, 4467.
(33) Lipatov, Y. S.; et al. *Polymer* **2002**, *43*, 875.
(34) Sinha Ray, S.; et al. *Polymer* **2004**, *45*, 8403.
(35) Li, Y.; Shimizu, H. *Polymer* **2004**, *45*, 7381.
(36) Gubbels, F.; et al. *Macromolecules* **1995**, *28*, 1559.
(37) Yurekli, K.; et al. *Macromolecules* **2003**, *36*, 7256.
(38) Khatua, B. B.; et al. *Macromolecules* **2004**, *37*, 2454.
(39) Ginzburg, V. V. *Macromolecules* **2005**, *38*, 2362.
(40) Balazs, A. C.; et al. *Science* **2006**, *314*, 1107.
(41) Poulin, P. *Science* **2005**, *309*, 2174.
(42) Gam, S.; et al. *Soft Matter* **2011**, *7*, 7262.
(43) Pieranski, P. *Phys. Rev. Lett.* **1980**, *45*, 569.
(44) Chung, H. J.; et al. *Macromolecules* **2007**, *40*, 384.
(45) Shull, K. R.; et al. *Macromolecules* **1991**, *24*, 2748.
(46) Leibler, L;et al. in *Ordering in Macromolecular Systems*; Teramoto, A, Norisuje, M. K. T., Eds.; Springer-Verlag, Berlin, 1994.
(47) Gam, S.. Ph.D. Dissertation, University of Pennsylvania, 2011.
(48) Shull, K. R. *Macromolecules* **1996**, *29*, 8487.
(49) de Gennes, P. G. *Macromolecules* **1980**, *13*, 1069.
(50) Gianetti, E. *Polym. Int.* **2001**, *50*, 10.
(51) Koberstein, J. T. *J. Polym. Sci., Part B: Polym. Phys.* **2004**, *42*, 2942.